

~~SECURITY INFORMATION~~

231

~~CONFIDENTIAL~~

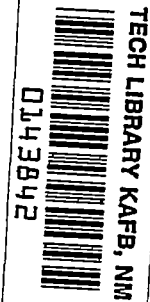
Copy  
RM L52C24

NACA RM L52C24

7317

~~CONFIDENTIAL~~

# NACA

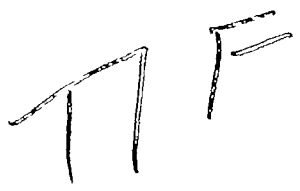


## RESEARCH MEMORANDUM

SKIN-FRICTION DRAG AND BOUNDARY-LAYER TRANSITION ON A  
PARABOLIC BODY OF REVOLUTION (NACA RM-10) AT A  
MACH NUMBER OF 1.6 IN THE LANGLEY 4- BY  
4-FOOT SUPERSONIC PRESSURE-TUNNEL

By K. R. Czarnecki and Jack E. Marte

Langley Aeronautical Laboratory  
Langley Field, Va.

  
CLASSIFIED DOCUMENT

~~CONFIDENTIAL~~

### NATIONAL ADVISORY COMMITTEE FOR AERONAUTICS

WASHINGTON

May 20, 1952

~~CONFIDENTIAL~~

30698/12

Classification cancelled (or changed to) Unclassified.....)

By Authority of AAA. A. Recon. Abn. Movement  
(OFFICER AUTHORIZED TO CHANGE)

74 30 NOV 54

By.....

GRADE OF OFFICER MAKING CHANGE

1072s (6)

GATE



## NATIONAL ADVISORY COMMITTEE FOR AERONAUTICS

## RESEARCH MEMORANDUM

SKIN-FRICTION DRAG AND BOUNDARY-LAYER TRANSITION ON A

PARABOLIC BODY OF REVOLUTION (NACA RM-10) AT A

MACH NUMBER OF 1.6 IN THE LANGLEY 4- BY

4-FOOT SUPERSONIC PRESSURE TUNNEL

By K. R. Czarnecki and Jack E. Marte

## SUMMARY

An investigation has been made at a Mach number of 1.6 and over a Reynolds number range from  $2 \times 10^6$  to  $40 \times 10^6$  of the skin-friction drag and boundary-layer transition of a body of revolution. The body had a parabolic-arc profile, a blunt base, and a fineness ratio of 12.2 (NACA RM-10). The results indicate the boundary layer remained essentially laminar over the entire length of the model, including a region of adverse pressure gradient near the base, up to a Reynolds number of about  $11 \times 10^6$ . Boundary-layer transition was very sensitive to surface condition and often occurred at lower Reynolds numbers if the surface was not maintained aerodynamically clean. A comparison of the boundary-layer transition results with those of other facilities shows that wind-tunnel turbulence or other flow irregularities have a large effect on transition at supersonic speeds.

## INTRODUCTION

In order to realize long ranges for airplanes and missiles at supersonic speed, fuselage bodies of high fineness ratios must be used. For such bodies the skin friction may compose a major part of the total drag, hence, knowledge of the magnitude of the skin friction is of great importance in calculating performance. In addition, a knowledge of the skin friction aids in predicting the effects of aerodynamic heating. One of the major problems in estimating skin friction or aerodynamic heating, however, lies in the difficulty of predicting at what point on the body transition from laminar to turbulent boundary layer flow will occur. The National Advisory Committee for Aeronautics, consequently, has

undertaken a general investigation of skin friction and boundary-layer transition at supersonic speeds. One phase of this general investigation consists of a coordinated research program to evaluate the scale effect on a parabolic-body research missile known as the NACA RM-10. Various scale models of this missile have been tested in NACA supersonic wind tunnels (references 1 to 3), and both full- and half-scale models have been tested in free flight (reference 4). The use of both wind-tunnel and free-flight test facilities has enabled data to be obtained at a few widely scattered intervals over a wide range of Reynolds numbers; for example,  $2.6 \times 10^6$  to  $90 \times 10^6$  at a Mach number of 1.6. In general, these studies of skin friction and boundary-layer transition were limited to an angle of attack of  $0^\circ$ .

This present paper presents results obtained on an RM-10 model at a Mach number of 1.6 in the repowered Langley 4- by 4-foot supersonic pressure tunnel, which allowed the Reynolds number to be varied continuously from about  $2 \times 10^6$  to about  $40 \times 10^6$ . Tests were made at zero angle of attack with natural and artificially fixed transition and a comparison is made of the results with other existing data.

#### SYMBOLS

A	maximum cross-sectional area of body
$C_D$	drag coefficient $\left(\frac{\text{Drag}}{qA}\right)$
M	free-stream Mach number
P	pressure coefficient $\left(\frac{p - p_o}{q_o}\right)$
$p_o$	free-stream static pressure
p	local static pressure
q	free-stream dynamic pressure $\left(\frac{\gamma}{2} p_o M^2\right)$
R	Reynolds number based on body length and free-stream velocity
u	velocity inside boundary layer
U	velocity just outside of boundary layer

$x/L$	distance from nose of model in body lengths
$y$	distance normal from body surface
$\gamma$	ratio of specific heats for air (1.4)
$\theta_1$	incompressible boundary-layer momentum thickness $\left( \int_0^\infty \frac{u}{U} \left( 1 - \frac{u}{U} \right) dy \right)$

## Subscripts:

$f$	skin friction
$F$	forebody pressure drag
$B$	average base

## APPARATUS AND METHODS

## Wind Tunnel

The present investigation was conducted in the Langley 4- by 4-foot supersonic pressure tunnel which is a rectangular, closed-throat, single-return type of wind tunnel with provisions for the control of the pressure, temperature, and humidity of the enclosed air. Changes in test-section Mach number are obtained by deflecting the top and bottom walls of the supersonic nozzle against fixed interchangeable templets which have been designed to produce uniform flow in the test section. With the recent installation of new and more powerful drive motors the tunnel operating range is from about  $1/8$  to  $2\frac{1}{4}$  atmospheres stagnation pressure over a nominal Mach number range from 1.2 to 2.2. The turbulence level of the tunnel is as yet undetermined. For qualitative visual-flow observation, a schlieren optical system is provided.

For the tests reported herein the nozzle walls were set for a Mach number of 1.6. At this Mach number, the test section has a width of 4.5 feet and a height of 4.4 feet. During the tests, the dew point was kept from below  $-35^\circ$  F at the lowest stagnation pressure to below  $-20^\circ$  F at the highest values so that the effects of water condensation in the supersonic nozzle were negligible.

## Model

A sketch of the RM-10 model, giving pertinent dimensions and construction details, is shown in figure 1 and a photograph of the model is presented as figure 2. The body has a parabolic-arc profile with a basic fineness ratio of 15. The pointed stern has been cut off at 81.25 percent of the length, however, so that the actual body has a blunt base and a fineness ratio of 12.2. The present model has a length of 50 inches and a maximum diameter of 4.096 inches.

The model was constructed of steel and duralumin in four sections. The joints between the sections were carefully sealed and faired until no discontinuity at the surface could be detected. Body contours are estimated to be accurate to within about 0.006 inch on the average, with a maximum deviation of 0.020 inch. The original surface roughnesses as determined by a Brush surface analyzer were about 6 root-mean-square microinches on the steel sections and about 14 root-mean-square microinches on the duralumin parts with maximum peak to valley roughnesses of 12 and 50 microinches for the respective metals. Most of the tests were made, however, with the model painted, sanded, waxed, and polished to an average surface roughness considerably less than that for the model in the original surface condition. No reliable measurements of the roughness of this surface could be obtained because the stylus cut too deeply into the soft surface. The surface was not so soft, however, as to be affected in any way during the tests insofar as demonstrated by repeatability of the results.

The body was mounted in the tunnel by means of a sting, and total drags were measured on an electrical strain-gage balance mounted within the model. Base pressures were determined from four 0.040-inch outside-diameter tubes placed on the sting with the openings in the plane of the base at 90° intervals around the sting. Boundary-layer profiles were determined by means of a rake of tubes illustrated in figures 1 and 3. In order to keep the lag in response of the rake within reasonable limits and yet obtain a sufficient number of point measurements within the thinner boundary layers, the rake was constructed of 0.040-inch outside-diameter (0.030 I.D.) tubing, but the ten tubes closest to the surface were flattened to a height of about 0.025-inch outside diameter (0.015 I.D.) per tube. The rake was clamped on the sting so that boundary-layer profiles were determined about 1/64 inch ahead of the base of the model. A few check tests were also made with a boundary-layer rake similarly constructed of 0.030-inch outside-diameter (0.020 I.D.) tubing. For the boundary-layer velocity-profile tests, the back end of the model was blocked up with wooden wedges to prevent any motion of the model relative to the rake. No other data were recorded at the time these data were obtained.

## Techniques, Tests and Data Reduction

During the investigation, base pressures were read simultaneously with the results from the strain-gage balance. For most test conditions, schlieren photographs were also made to aid in interpreting results. No photographs are presented in this paper, however, because they lacked sufficient detail for satisfactory reproduction.

Tests were made with the model in the original smooth condition; in the painted, sanded, waxed, and polished condition; and with transition fixed. Fixing transition was accomplished by means of a circumferential ring of number 60 carborundum grains located a half-inch back from the nose and about  $1/4$  inch wide in the direction of the flow. The grains covered roughly  $1/5$  to  $1/4$  of the surface area within the ring.

The tests were made with the model at zero angle of attack and in temperature equilibrium. The tunnel stagnation pressure was varied from 2 to 33 pounds per square inch which gave a Reynolds number range, based on the model length of 50 inches, from about  $2 \times 10^6$  to  $40 \times 10^6$ .

The total drag was determined from strain-gage measurements and the base drag from base pressures. No bouyancy corrections arising from small static-pressure gradient in the test section were applied as calculation showed the correction to be well within the experimental accuracy.

In order to determine the skin-friction drag of a body by this technique, the forebody pressure drag must be known. Inasmuch as past experience has indicated that the forebody pressure drag varies very little with Reynolds number, especially when the boundary layer remains laminar or stays turbulent near the base, the forebody pressure drag was not determined in this investigation but was taken from the experimental results presented in reference 3 for a geometrically similar but slightly smaller model. These forebody-pressure-drag coefficients were, according to the reference, 0.041 when the boundary layer was essentially laminar and 0.044 when the boundary layer was made turbulent by fixing transition. A plot of the pressure distributions from which the coefficients were derived is shown in figure 4. The plot also shows the extent of the favorable pressure gradient over the body. It was assumed that the above values of forebody-pressure-drag coefficient did not vary with Reynolds number except to change from the laminar to turbulent values in the Reynolds number range near  $10 \times 10^6$ . This range was chosen on the basis of skin-friction and boundary-layer-profile results which are discussed subsequently. In actuality, the transition in forebody-pressure-drag coefficients probably will not be as abrupt as assumed but the actual variation is not known and, in any case, the

difference between the coefficients is small. With transition fixed,  $C_{D_F}$  was assumed constant at the turbulent values of 0.044. With the forebody pressure drag thus estimated, the skin-friction drag was determined by subtracting the base and estimated forebody pressure drags from the total drag.

Skin-friction coefficients from the boundary-layer-pressure data were obtained by the loss in momentum technique outlined in reference 5 together with an assumed temperature recovery factor of 0.88, a value reasonably applicable to both laminar and turbulent flow.

#### Precision of Data

Stream surveys obtained at tunnel stagnation pressures of 15 and 30 pounds per square inch with empty test section indicate that, in general, the mean value of Mach number in the region occupied by the model in the test nozzle was 1.61 and that the variation about this mean was less than 0.6 percent (fig. 5). Some evidence (wall static pressures) of a slight decrease in test-section Mach number was found for tunnel stagnation pressures of about 4 pounds per square inch and below, but sufficient data are lacking to establish the accuracy of this indication for the flow at the center of the test section. Calculations showed that the effect of the decreased Mach number on the aerodynamic coefficients was small. No significant irregularities in stream-flow direction in the region occupied by the model were found to exist.

The various coefficients presented in the paper are estimated to be accurate within the following limits:

Drag coefficient $C_D$ . . . . .	$\pm 3$ to $\pm 4$ percent
Forebody pressure drag coefficient $C_{D_F}$ . . . . .	$\pm 0.003$
Base drag coefficient $C_{D_B}$ . . . . .	$\pm 0.001$
Skin-friction drag coefficient $C_{D_f}$ . . . . .	$\pm 0.004$
Base pressure coefficient $P_B$ . . . . .	$\pm 0.003$

### RESULTS AND DISCUSSION

#### Effects of Surface Condition

The basic results of the drag investigation of the RM-10 body over the Reynolds number range are shown in figures 6 to 9 for the model in the smooth condition and with boundary-layer transition fixed near the



nose. Initially, smooth-model tests were made with only normal precautions to keep the model clean. A rather large scattering of data occurred in the Reynolds number range where the skin-friction drag coefficient increased abruptly with  $R$  (that is, in the Reynolds number range from  $7 \times 10^6$  to  $15 \times 10^6$ ) and test points often could not be repeated. Because of these undesirable conditions, the model was carefully cleaned before each run. After testing through the Reynolds number range in the carefully cleaned condition for both increasing and decreasing Reynolds numbers, the model surface was refinished as smooth as possible by painting, sanding, waxing, and polishing and tested again in each direction through the Reynolds number range. Identical results were obtained for both surface conditions with large scale scatter eliminated; hence, the test points for the two surface conditions are not differentiated on the plots and the earlier scattered data are omitted. In many instances the omitted data showed larger values of total, skin friction and base drag than are shown in figures 6 to 9, indicating the occurrence of boundary-layer transition at lower values of  $R$  when the model was not aerodynamically clean.

#### Drag Breakdown

Total drag.— The variation of total drag coefficient with Reynolds number for carefully cleaned models, with and without artificial transition, is shown in figure 6. In the smooth surface conditions the total drag coefficient decreased slowly with increase in Reynolds number up to a Reynolds number of about  $7 \times 10^6$  (see fig. 6(a)). At this point, the total drag coefficient increased abruptly from about 0.068 to 0.088 and thence remained approximately constant to about  $R = 10 \times 10^6$ . Above the latter Reynolds number, the total drag coefficient again increased, rapidly at first and more gradually later, until a Reynolds number of perhaps  $30 \times 10^6$  to  $35 \times 10^6$  was attained. With further increases in Reynolds number, the total drag coefficient remained fairly constant and perhaps finally began to decrease.

With transition fixed (fig. 6(b)), the total drag coefficient was generally much higher at the lower Reynolds number and decreased slowly and continuously over the complete test Reynolds number range as contrasted with the abrupt changes characteristic of the smooth model. At a Reynolds number in the neighborhood of  $35 \times 10^6$  the drag coefficient for the smooth model and for the model with transition fixed tended to become equal (compare figs. 6(a) and 6(b) extrapolated), the indication being that natural transition was occurring near the nose of the model. In reaching this conclusion, it was assumed that the roughness did not significantly change the character of the boundary layer other than by initiating transition.

Base pressure coefficient and drag.- The average base pressure and corresponding base drag coefficients determined on the RM-10 in this investigation are presented in figure 7. The results indicate that, in the smooth-surface conditions, the base pressure at the lowest Reynolds numbers investigated was only slightly negative, hence, the base drag was small. As the Reynolds number was increased, however, the base pressure decreased sharply at  $R = 7 \times 10^6$ , the point at which the total drag coefficient had increased abruptly, and thence continued to decrease at a somewhat slower rate up to  $R = 11 \times 10^6$ . The corresponding increase in  $C_{DB}$  was from about 0.006 at  $R \approx 6 \times 10^6$  to 0.036 at  $R \approx 11 \times 10^6$ . From  $R = 11 \times 10^6$  to  $R = 19 \times 10^6$  the base pressure coefficient increased and then began to decrease slowly with further increase in Reynolds number with  $C_{DB}$  reaching a value of about 0.035 at the highest values of  $R$  investigated.

With transition fixed the abrupt changes in base pressure were eliminated and the base pressure continuously and gradually decreased with Reynolds number over the test Reynolds number range from  $4 \times 10^6$  to  $27 \times 10^6$ . Above a Reynolds number of about  $19 \times 10^6$  the base pressure coefficient  $P_B$  and, hence, the base drag coefficient  $C_{DB}$  for the transition-fixed condition were essentially the same as those for the smooth model.

Skin-friction drag.- The differences in drag between the curves of total drag coefficient and forebody plus base-pressure drag coefficient in figure 6 indicate the magnitude of the skin-friction coefficient. An analysis of the results for the smooth model shows that in the essentially laminar flow regime the skin friction comprised one-third of the total drag; in the case where the basically turbulent boundary layer covered most of the model (natural transition near nose of model at  $R = 30 \times 10^6$ ), the skin friction amounted to one-half of the total drag. When transition was artificially fixed, the skin friction contributed about half of the total drag over the entire test Reynolds number range, with the ratio of skin friction to total drag being slightly higher at the lower end of the Reynolds number range.

A plot of the skin-friction drag derived from the data in figure 6 is presented in figure 8 on a logarithmic scale. Included in the figure are all skin-friction drags available to date on the RM-10 at  $M \approx 1.6$ . The results of the present investigation indicate that the boundary layer remained essentially laminar over the entire length of the model, including the region of adverse pressure gradient near the base, up to a Reynolds number of about  $11 \times 10^6$ . At this point the main

drag rise due to boundary layer transition began and, with further increase in Reynolds number, transition moved forward progressively until at  $R = 35 \times 10^6$  to  $40 \times 10^6$  it apparently occurred close to the nose of the model. In correlating the present skin-friction results with the base coefficients, it is noted that the beginning of the main drag rise due to transition at  $R = 11 \times 10^6$  (fig. 8) apparently coincides with the peak of the pressure bump in the  $P_B$  curve (fig. 7).

Since the experimental skin-friction drag increased so rapidly above  $R = 11 \times 10^6$ , an analysis was made on the basis of the transition curve (fig. 8) of the transition Reynolds numbers based on the distance from the model apex to the point where transition occurred. The calculations reveal that this transition Reynolds number decreased gradually from about  $11 \times 10^6$  to approximately half this value or less as the test Reynolds number based on body length increased from  $11 \times 10^6$  to  $40 \times 10^6$  even though the transition region progressively moved forward into the influence of a more and more favorable pressure gradient. At the present time, sufficient data are lacking to determine whether the apparent decrease in transition Reynolds number with increase in tunnel pressure is precipitated by an increase in tunnel turbulence level with increase in stagnation pressure or is influenced by some factor such as the increased surface-roughness to boundary-layer-thickness ratio near the model nose.

The present data agree fairly well with those obtained at low Reynolds numbers for a smaller RM-10 model in the Langley 4- by 4-foot tunnel before it was repowered and with some results obtained in the Langley 9-inch supersonic tunnel. The same forebody pressure drag was used in reducing data in these instances. At the higher Reynolds number of  $30 \times 10^6$  the present results are in good agreement with the skin-friction data obtained on an RM-10 in the Lewis 8- by 6-foot tunnel (reference 1); whereas a comparison of the present results with those obtained at  $M = 1.52$  on an RM-10 in the Ames 1- by 3-foot tunnel (reference 2) indicates that boundary-layer transition in that facility apparently occurred at much lower Reynolds numbers than in the present investigation. The existence of the discrepancy probably can be ascribed to the effects of wind-tunnel turbulence (the Ames 1- by 3-foot tunnel is a butterfly-valve controlled blowdown tunnel with smaller contraction ratio than the Langley 4- by 4-foot supersonic pressure tunnel) or other flow irregularities (for example, compare the Mach number variations of  $\pm 0.01$  in present tests to  $\pm 0.02$  in the Ames investigation). The comparison appears to show that the problem of turbulence in supersonic wind tunnels is important, just as it is in low-speed wind tunnels, and points out the need for establishing wind-tunnel turbulence levels and eliminating any large flow disturbances before any significant

analysis of skin friction, base pressure, boundary-layer transition, and shock-boundary layer interaction can be made at supersonic speeds within the Reynolds number ranges now under investigation.

The skin-friction results obtained in free flight by means of boundary-layer surveys on full-scale models at  $R = 85 \times 10^6$  (unpublished) and  $R = 112 \times 10^6$  (reference 5) are not in too good an agreement with the extrapolated curve of the present investigation. Too much importance should not be placed upon this comparison, however, as the heat-transfer conditions for these flight-test points correspond to those of a skin far colder than that existing for the zero-heat-transfer conditions of the wind-tunnel data. A theory for the effect of heat transfer on skin friction in turbulent boundary layers formulated by Van Driest (for example, reference 6) accounts for approximately one-third of the difference between the flight-test points and the tunnel results extrapolated along the turbulent curve.

In general, the present experimental skin-friction coefficients were in good agreement with the theoretical coefficients computed with the aid of Manglers transformation (reference 7) and with the parabolic profile of the body taken into account. The basic flat-plate boundary-layer theories used to make the calculations were the Chapman and Rubesin theory (reference 8) for laminar boundary layers and the extended Frankl and Voishal method (reference 9) for turbulent boundary layers. For laminar flow, the calculations indicate an increase of 9 percent in skin-friction for the RM-10 over that of a flat plate. With a turbulent boundary layer, the increase in skin friction is only about 2 percent. Recently, Van Driest (reference 6) derived a relationship between the turbulent skin friction on a cone relative to that on a flat plate which, when applied to the Reynolds number range of interest here, indicated an increase in cone skin friction of 12 to 13 percent. For a parabolic body the increase will be somewhat less. The experimental data, however, appear to be in better agreement with the smaller increase indicated by Manglers transformation.

#### Results of Boundary-Layer Surveys

Velocity profiles.— The boundary-layer velocity profiles determined at the base are presented in figure 9. At the lower Reynolds numbers where the boundary layer was regarded as laminar at the base of the model, the total pressure nearest the surface was higher than the total pressure immediately further out, so that a high calculated velocity ratio resulted near the surface. This effect was also found with a pressure tube rake made from 0.030-inch outside-diameter tubing. This apparent excess of total pressure may be the result of the tube nearest the surface being in a large total pressure gradient, the rake being

located too close to the base of the body, or boundary-layer separation. The use of the usual correction factors for tubes close to the surface (reference 10) did not lead to any significant improvements in the velocity distributions, hence, the corrections have not been incorporated in the data of figure 9. It is difficult to foresee how the location of the rake too near the base or boundary-layer separation could result in high total pressures near the surface but the pressure data of figure 4 do indicate the possibility of flow separation near the base of the body when the boundary layer is laminar and the pressure tube rake itself may have induced separation. Since it is not known which one, if any, of the above factors is responsible for the high readings of the tube nearest the surface, the data from that tube were disregarded in fairing the boundary-layer profiles and the integrated skin-friction results may, therefore, be somewhat questionable. This uncertainty, however, should have no effect on the qualitative value of the results.

In any event, up to  $R = 9.2 \times 10^6$  the nondimensional experimental velocity profiles are all practically identical and have characteristics very similar to those of the Blasius profile, except for a small displacement of the experimental profile to smaller values of  $y/\theta_1$

(fig. 9). At Reynolds numbers of  $11.3 \times 10^6$  or greater the experimental profiles are again identical in shape but the high total pressures near the surface have disappeared and the profiles have more of the characteristics of turbulent-boundary-layer profiles. The best agreement of the experimental velocity profiles at high Reynolds numbers was found with an approximately  $\frac{1}{9}$ -power profile. The boundary-layer surveys thus show an apparent change from a laminar to turbulent boundary-layer profile and a change from decreasing to increasing momentum thickness  $\theta_1$  in the Reynolds number range between  $9.2 \times 10^6$  and  $11.3 \times 10^6$  which are characteristics of transition and in good agreement with the transition Reynolds number range indicated by the force tests.

Skin friction.- The skin-friction drag coefficients computed from the momentum loss in the boundary layer are plotted in figure 8. The results are in qualitative agreement with the force data as to both the point of beginning of boundary-layer transition and the relative magnitudes of the skin-friction coefficients with the boundary layers both laminar and turbulent.

#### SUMMARY OF RESULTS

An investigation has been made at a Mach number of 1.6 and over a Reynolds number range from  $2 \times 10^6$  to  $40 \times 10^6$  of the skin-friction

CONFIDENTIAL

drag and boundary-layer transition of a body of revolution. The body had a parabolic-arc profile, a blunt base, and a fineness ratio of 12.2 (NACA RM-10). The results indicate that:

1. The boundary layer remained essentially laminar over the entire length of the model, including a region of adverse pressure gradient near the base, up to a Reynolds number of about  $11 \times 10^6$ . At this point the main drag rise due to boundary-layer transition began and, with further increase in Reynolds number, transition moved forward progressively until at a Reynolds number of about  $35 \times 10^6$  to  $40 \times 10^6$  transition apparently occurred close to the nose of the model.
2. In the essentially laminar flow regime, the skin-friction comprised about one-third of the total drag; in the case in which the basically turbulent boundary layer covered most of the model, the skin friction amounted to one-half of the total drag.
3. Boundary-layer transition was very sensitive to surface condition and often occurred at lower Reynolds numbers if the surface was not maintained aerodynamically clean.
4. Wind-tunnel turbulence levels and other flow irregularities in supersonic wind tunnels appear to have a large effect on transition at supersonic speeds.
5. The magnitudes of skin-friction drag coefficients determined from boundary-layer profile measurements were in qualitative agreement with those obtained from force tests, and the pressure data substantiate the force test results as regards boundary-layer transition.

Langley Aeronautical Laboratory  
National Advisory Committee for Aeronautics  
Langley Field, Va.

## REFERENCES

1. Esenwein, Fred T., Obery, Leonard J., and Schueller, Carl F.: Aerodynamic Characteristics of NACA RM-10 Missile in 8- by 6-Foot Supersonic Wind Tunnel at Mach Numbers from 1.49 to 1.98. II - Presentation and Analysis of Force Measurements. NACA RM E50D28, 1950.
2. Perkins, Edward W., Gowen, Forrest E., and Jorgensen, Leland H.: Aerodynamic Characteristics of the NACA RM-10 Research Missile in the Ames 1- by 3-Foot Supersonic Wind Tunnel No. 2 - Pressure and Force Measurements at Mach Numbers of 1.52 and 1.98. NACA RM A51G13, 1951.
3. Hasel, Lowell E., Sinclair, Archibald R., and Hamilton, Clyde V.: Preliminary Investigation of the Drag Characteristics of the NACA RM-10 Missile at Mach Numbers of 1.40 and 1.59 in the Langley 4- by 4-Foot Supersonic Tunnel. NACA RM L52A14, 1952.
4. Jackson, H. Herbert, Rumsey, Charles B., and Chauvin, Leo T.: Flight Measurements of Drag and Base Pressure of a Fin-Stabilized Parabolic Body of Revolution (NACA RM-10) at Different Reynolds Numbers and at Mach Numbers from 0.9 to 3.3. NACA RM L50G24, 1950.
5. Rumsey, Charles B., and Loposer, J. Dan: Average Skin-Friction Coefficients from Boundary-Layer Measurements in Flight on a Parabolic Body of Revolution (NACA RM-10) at Supersonic Speeds and at Large Reynolds Numbers. NACA RM L51B12, 1951.
6. Van Driest, E. R.: Turbulent Boundary Layer on a Cone in a Supersonic Flow at Zero Angle of Attack. Jour. Aero. Sci., vol. 19, no. 1, Jan. 1952, pp. 55-57, 72.
7. Mangler, W.: Boundary Layers with Symmetric Airflow about Bodies of Revolution. Rep. No. R-30-18, Part 20, Goodyear Aircraft Corp., March 6, 1946.
8. Chapman, Dean R., and Rubesin, Morris W.: Temperature and Velocity Profiles in the Compressible Laminar Boundary Layer with Arbitrary Distribution of Surface Temperature. Jour. Aero. Sci., vol. 16, no. 9, Sept. 1949, pp. 547-565.
9. Rubesin, Morris W., Maydew, Randall C., and Varga, Steven A.: An Analytical and Experimental Investigation of the Skin Friction of the Turbulent Boundary Layer on a Flat Plate at Supersonic Speeds. NACA TN 2305, 1951.

10. Von Doenhoff, Albert E.: Investigation of the Boundary Layer about a Symmetrical Airfoil in a Wind Tunnel of Low Turbulence. NACA ACR, Aug. 1940.



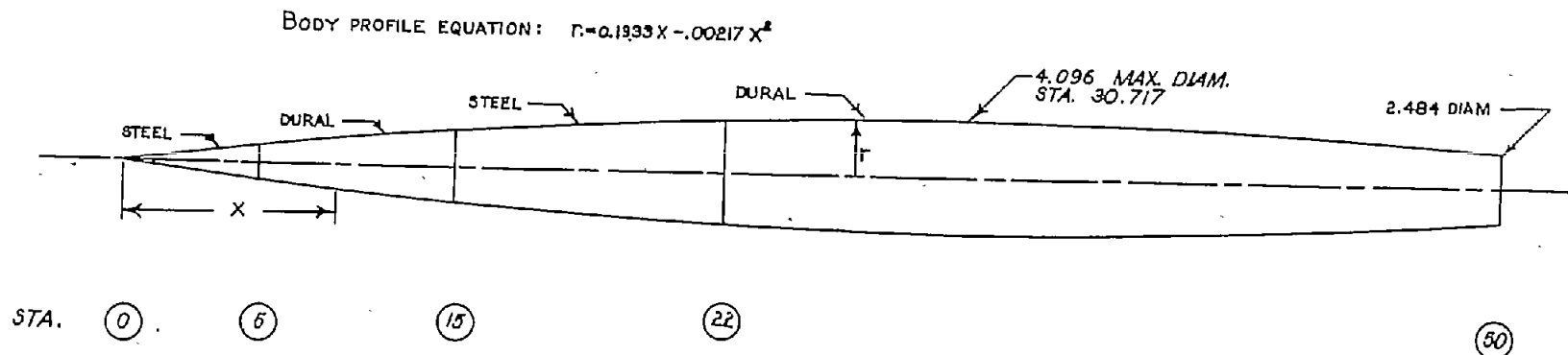


TABLE OF RAKE TUBE LOCATION

TUBE	DISTANCE - y
1	1.073
2	.760
3	.611
4	.522
5	.427
6	.341
7	.282
8	.253
9	.223
10	.194
11	.163
12	.134
13	.104
14	.073
15	.044
16	.016

ALL DIMENSIONS ARE IN INCHES

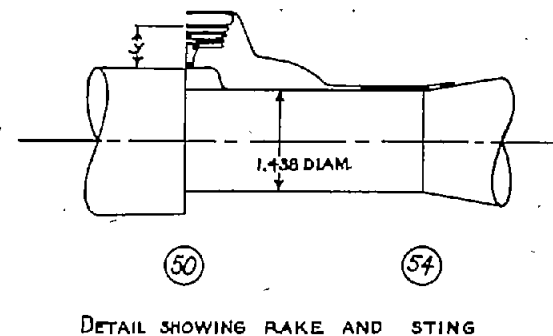
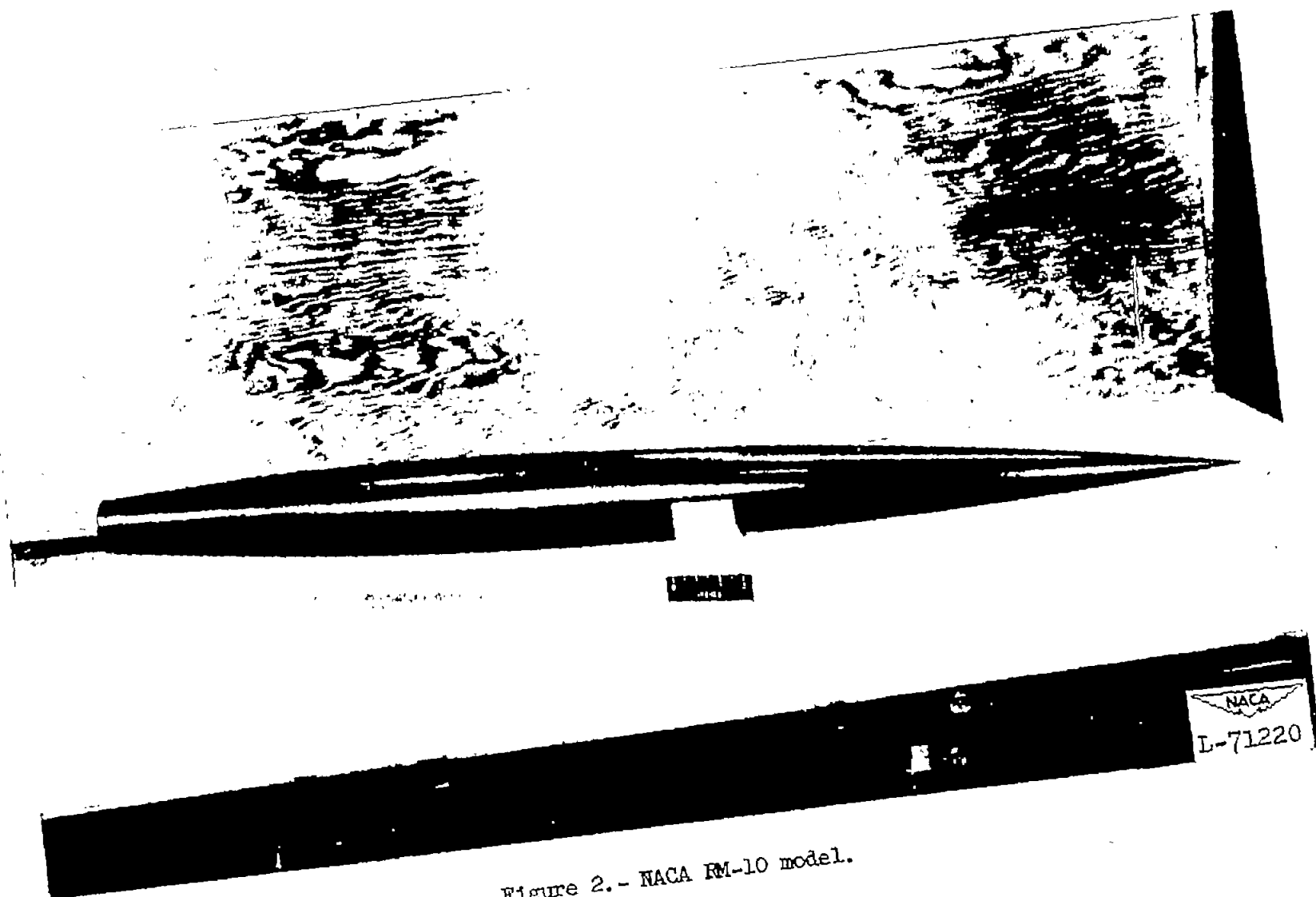


Figure 1.- General configuration and body equation of NACA RM-10 with detail of boundary-layer survey rake and table of tube locations.

CONFIDENTIAL



CONFIDENTIAL

Figure 2.- NACA RM-10 model.

NACA RM L52024

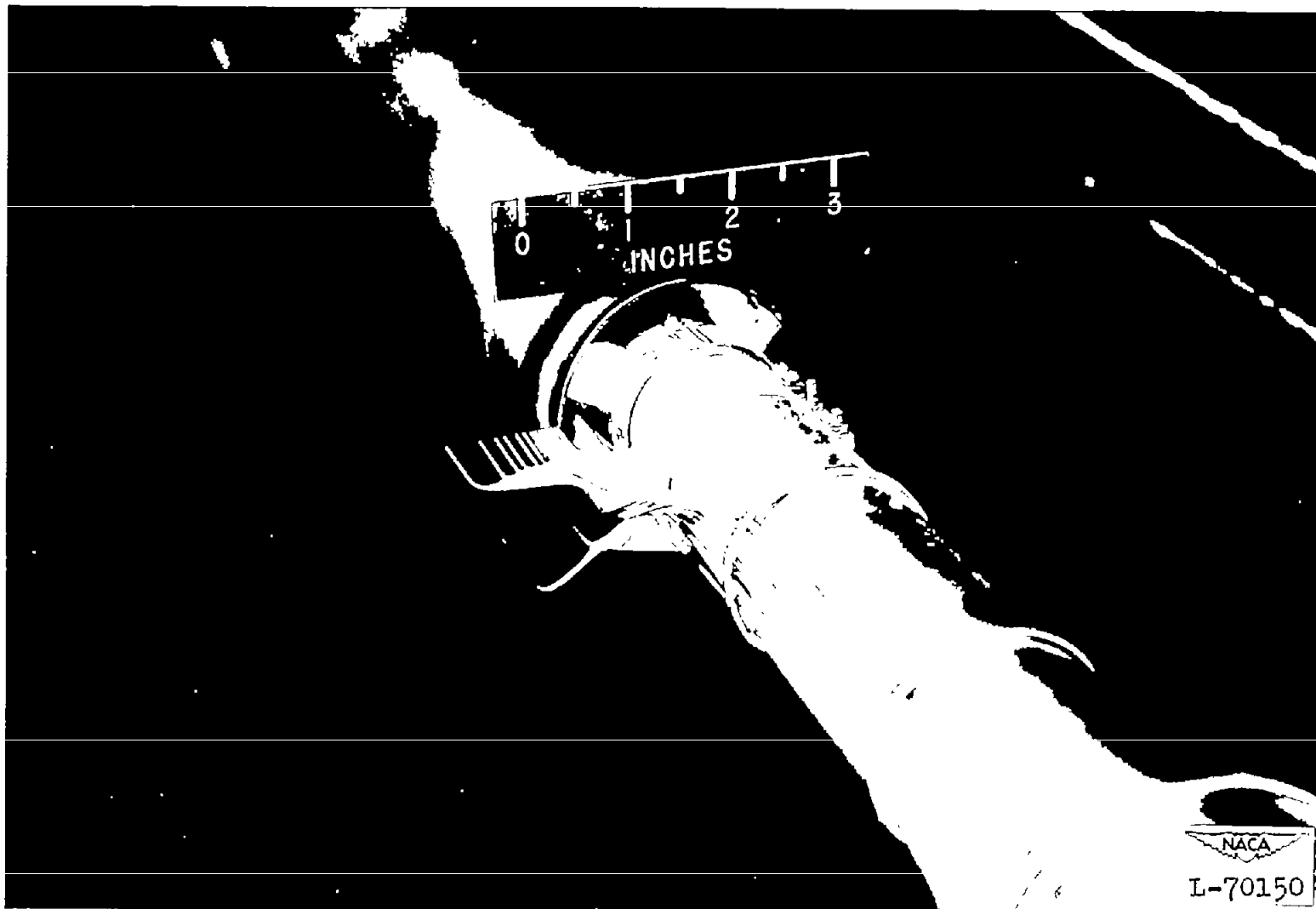


Figure 3.- Boundary-layer rake mounted at rear of model.

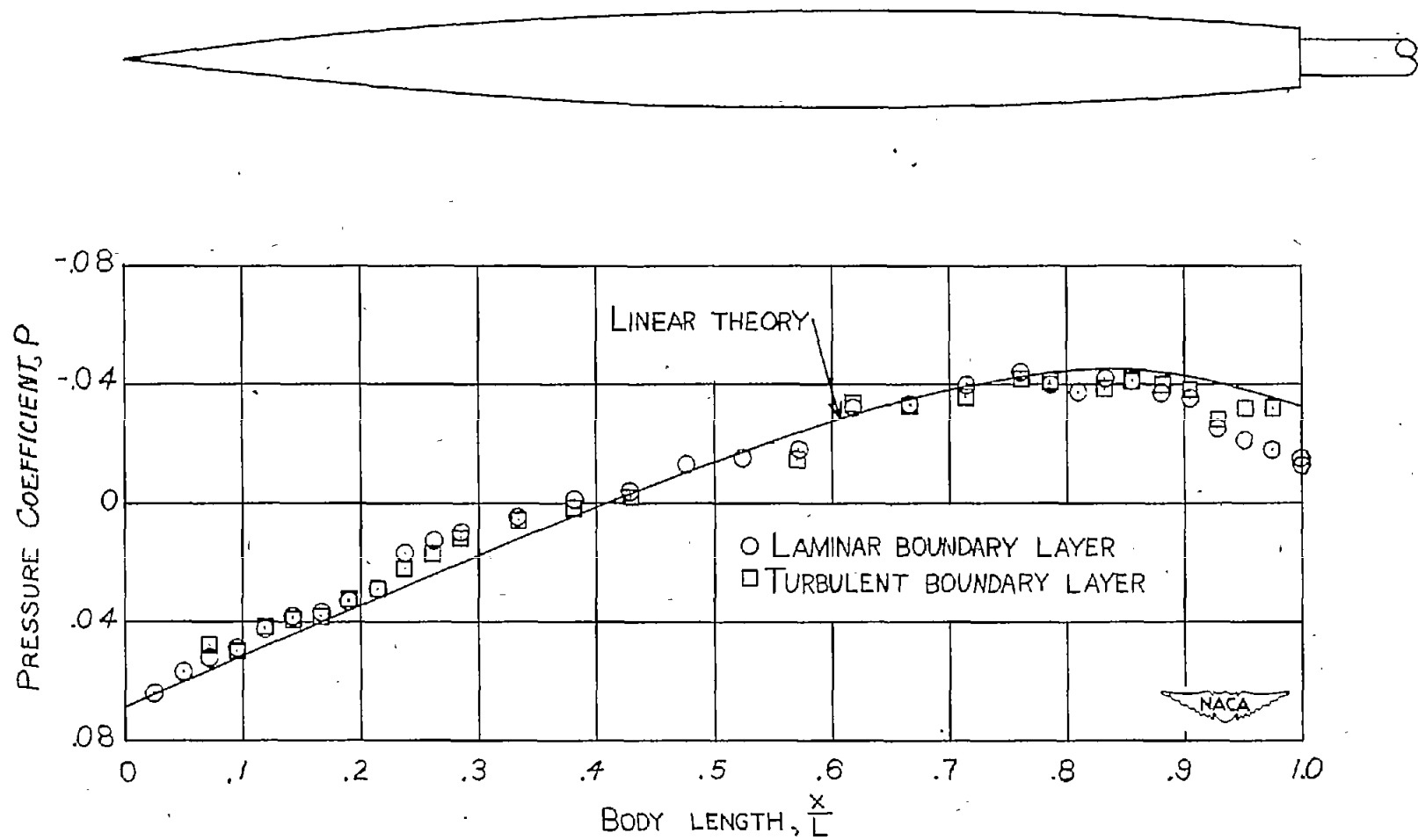


Figure 4.- Pressure distribution on NACA RM-10 at  $M \approx 1.6$  with laminar and turbulent boundary.

CONFIDENTIAL

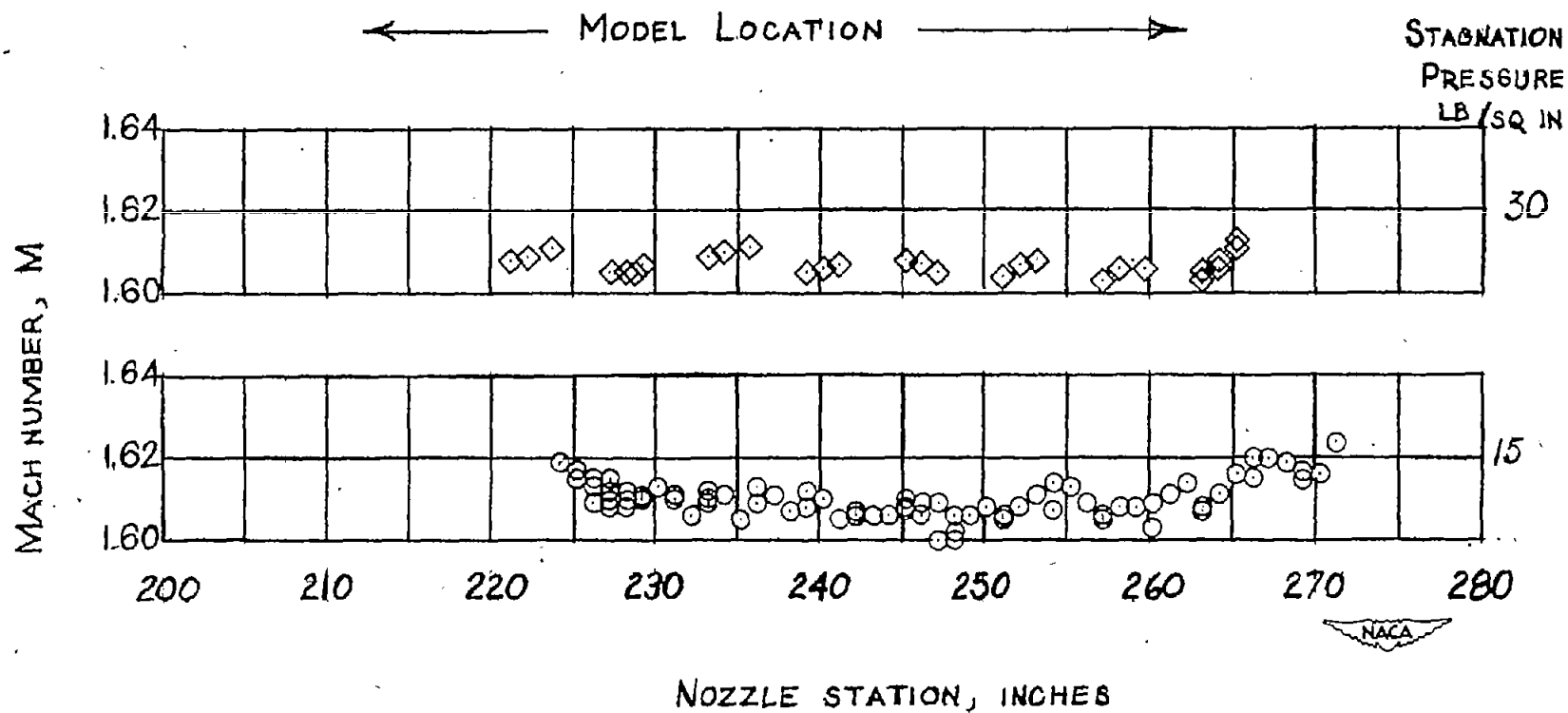
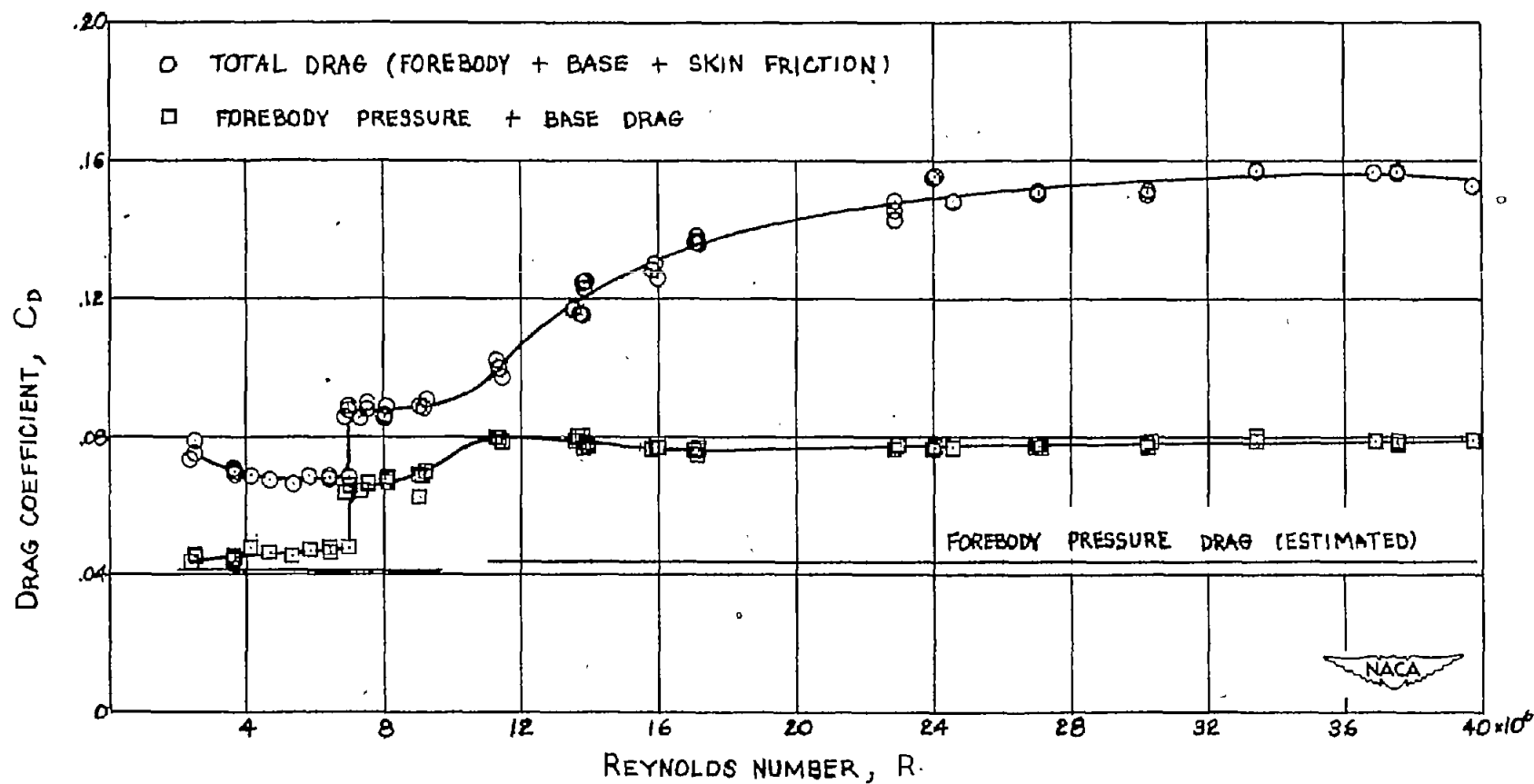
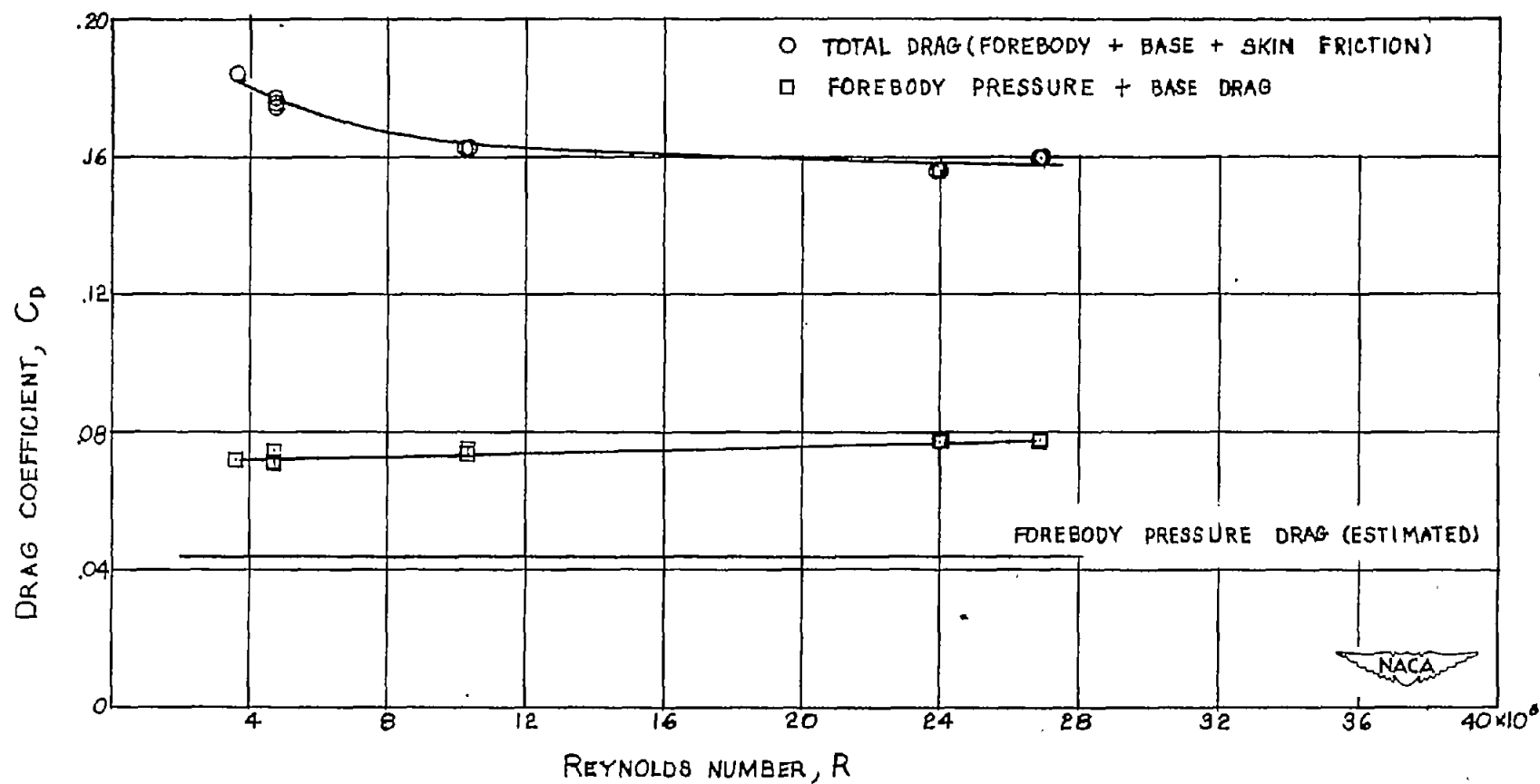


Figure 5.- Mach number distribution along test-section axis of the repowered Langley 4- by 4-foot supersonic pressure tunnel for different stagnation pressures.



(a) Smooth model.

Figure 6.- Variation of total and component drag coefficients with Reynolds number.



(b) Transition fixed.

Figure 6.- Concluded.

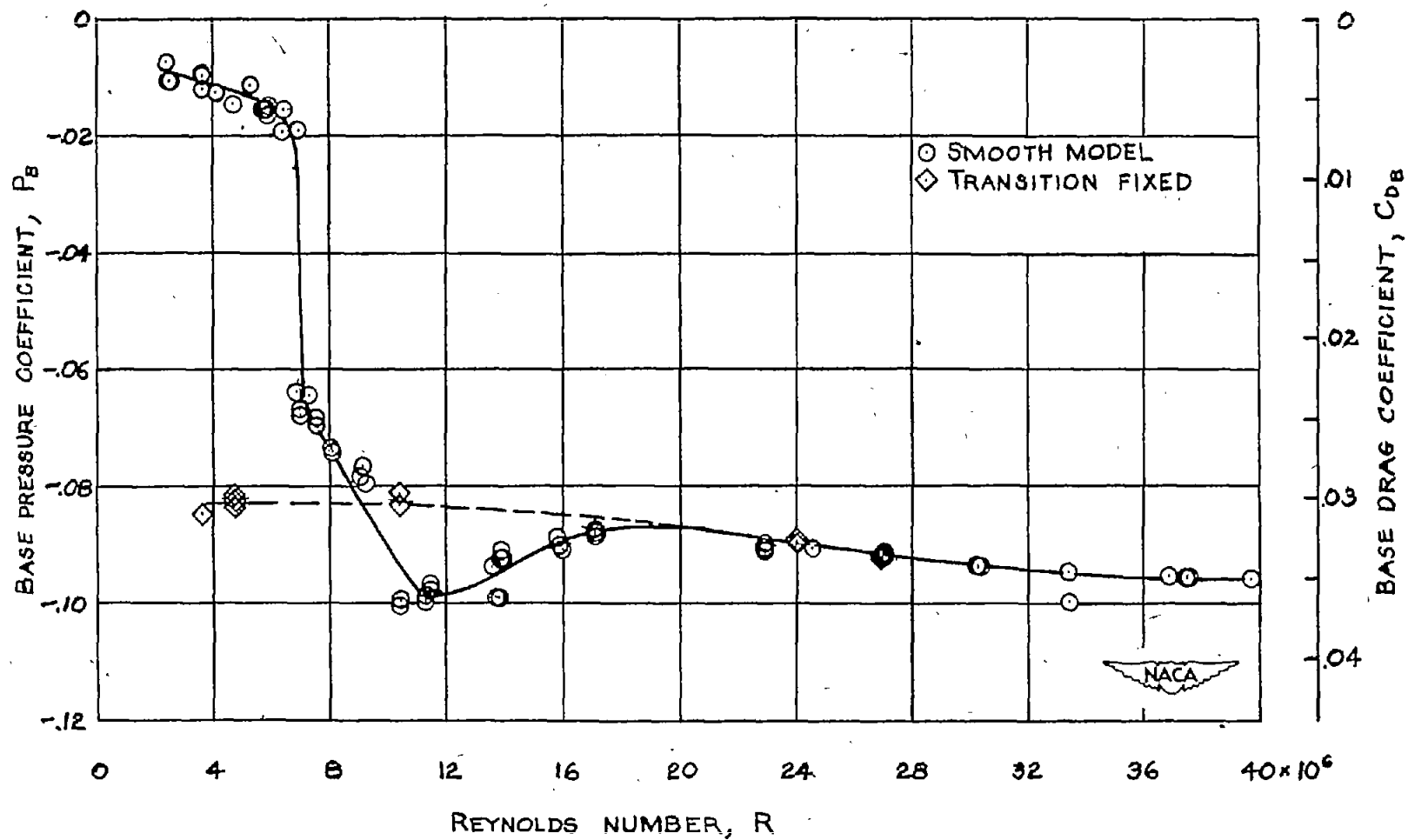


Figure 7.- Variation of base pressure and base drag coefficients with Reynolds number.



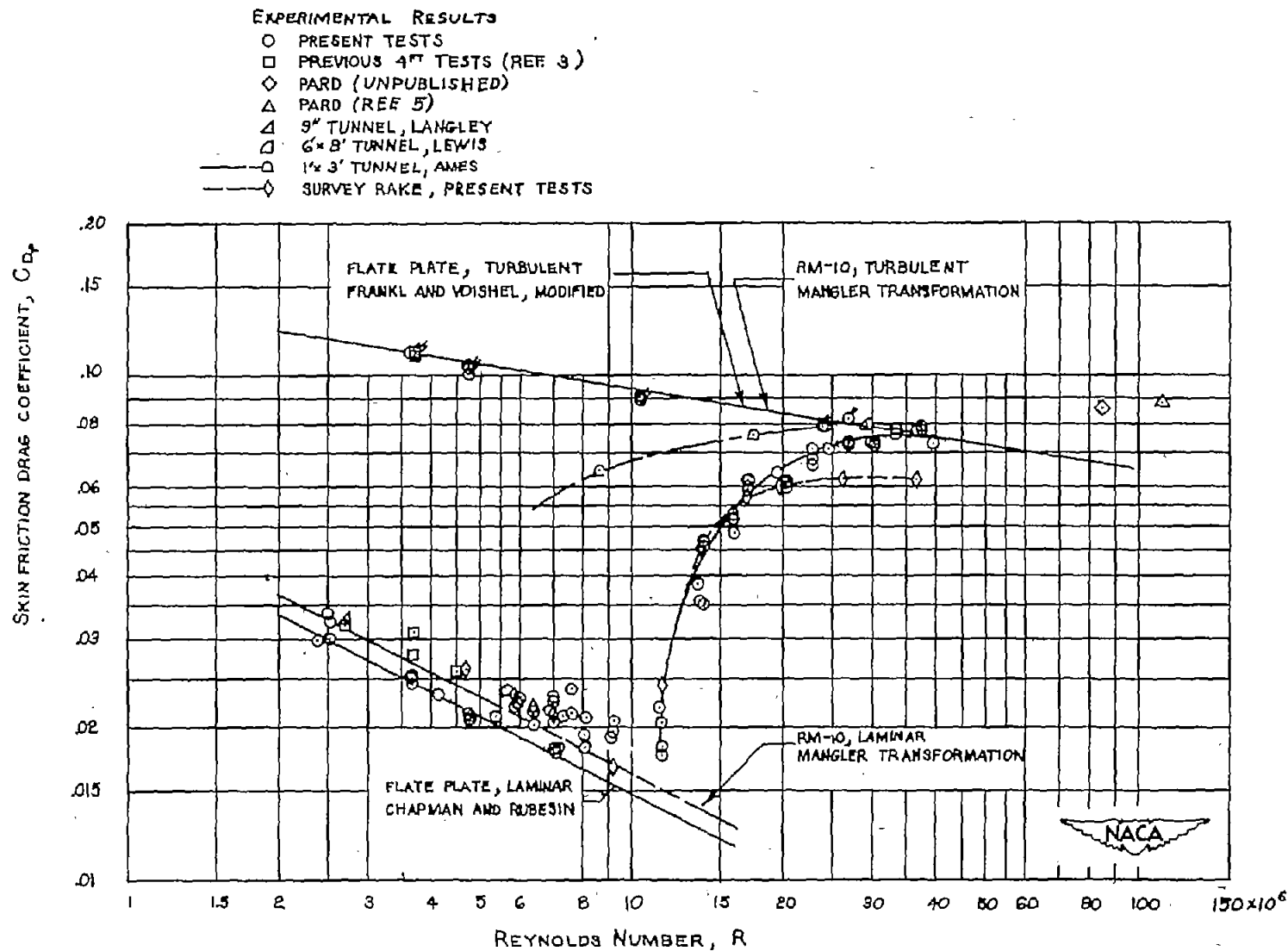


Figure 8.- Variation of skin-friction drag coefficient with Reynolds number and comparison with existing data for RM-10 at  $M \approx 1.6$ . (Flagged symbols indicate fixed transition.)

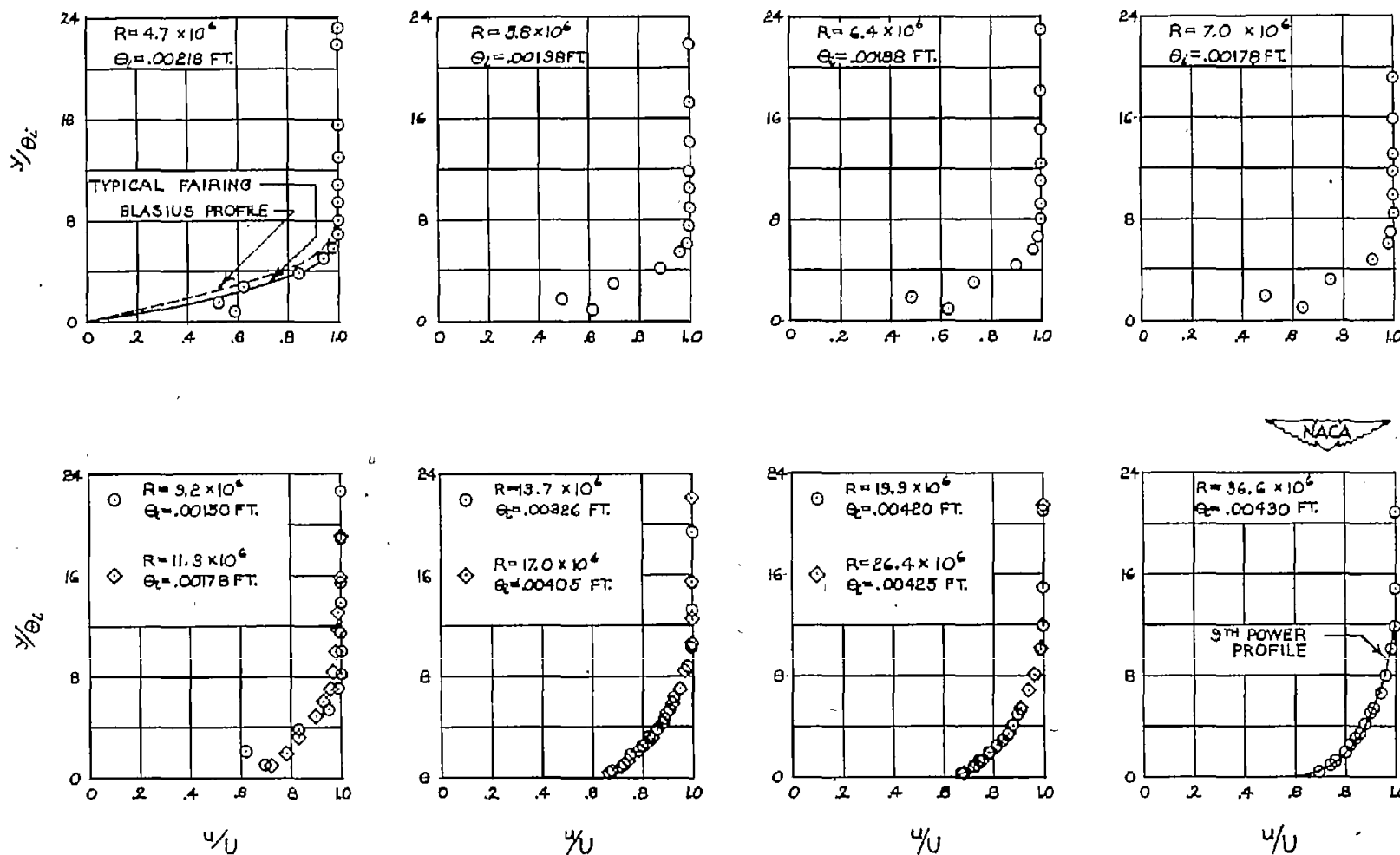


Figure 9.- Variation of nondimensional velocity profiles with Reynolds number.

CONFIDENTIAL

NACA RM L52C24

CONFIDENTIAL